# *On the local view of atmospheric available potential energy*

# On the Local View of Atmospheric Available Potential Energy

LENKA NOVAK AND RÉMI TAILLEUX

*Department of Meteorology, University of Reading, Reading, United Kingdom*

(Manuscript received 12 November 2017, in final form 12 February 2018)

ABSTRACT

The possibility of constructing Lorenz's concept of available potential energy (APE) from a local principle has been known for some time, but it has received very little attention so far. Yet the local APE density framework offers the advantage of providing a positive-definite local form of potential energy, which, like kinetic energy, can be transported, converted, and created or dissipated locally. In contrast to Lorenz's definition, which relies on the exact from of potential energy, the local APE density theory uses the particular form of potential energy appropriate to the approximations considered. In this paper, this idea is illustrated for the dry hydrostatic primitive equations, whose relevant form of potential energy is the specific enthalpy. The local APE density is nonquadratic in general but can nevertheless be partitioned exactly into mean and eddy components regardless of the Reynolds averaging operator used. This paper introduces a new form of the local APE density that is easily computable from atmospheric datasets. The advantages of using the local APE density over the classical Lorenz APE are highlighted. The paper also presents the first calculation of the three-dimensional local APE density in observation-based atmospheric data. Finally, it illustrates how the eddy and mean components of the local APE density can be used to study regional and temporal variability in the large-scale circulation. It is revealed that advection from high latitudes is necessary to supply APE into the storm-track regions, and that Greenland and the Ross Sea, which have suffered from rapid land ice and sea ice loss in recent decades, are particularly susceptible to APE variability.

## 1. Introduction

The stored potential energy that is available to fuel global circulation and the kinetic energy that quantifies that circulation are two key diagnostics that summarize the global state of the dynamical and thermodynamic properties of the atmosphere and oceans. As a result, these energies and the conversions between them are commonly diagnosed in global climate change and model verification studies (e.g., O'Gorman and Schneider 2008; Mbengue and Schneider 2017).

It has long been recognized that energy budgets are only useful if the potential energy (PE) is partitioned into its available (APE) and background ($PE_r$) components, following Lorenz's (1955b) pioneering work. Indeed, this is because there is often no direct correspondence between variations of potential energy and variations of kinetic energy, as in the case of the "cooling paradox," whereby cooling results in the creation of kinetic energy despite being a net sink of potential energy. In contrast, variations in APE are a much better predictor of variations in kinetic energy. However, a major difficulty with Lorenz's APE is that it is only defined in a global and volume-integrated sense. With an increasing emphasis of climate change research on regional variability in high-resolution climate models, there is an increasing need for locally definable diagnostics that can summarize large amounts of data.

While the local character of kinetic energy is already well established and widely used, the possibility to define APE from a local principle remains poorly known, despite it being proved over 30 years ago in two seminal papers by Andrews (1981) and Holliday and McIntyre (1981) for a compressible nonhydrostatic fluid and an incompressible fluid, respectively. This paper advocates the use of this local APE framework and demonstrates its applicability to the discussion of various aspects of atmospheric energetics in the context of the hydrostatic primitive equations for a dry atmosphere.

Available potential energy was first defined formally by Lorenz (1955b) as the difference between the total global potential energy of the actual state of the

Denotes content that is immediately available upon publication as open access.

*Corresponding author*: Lenka Novak, l.novakova@reading.ac.uk

DOI: 10.1175/JAS-D-17-0330.1

atmosphere and its adiabatically rearranged reference state. For a dry hydrostatic atmosphere viewed as a perfect gas and in absence of orography, one possible exact expression for Lorenz APE is as follows:

$$\overline{\mathrm{APE}_{\mathrm{Lor}}} = \frac{c_p}{g p_0^{\kappa}} \frac{1}{(1+\kappa)} \int_0^{\infty} \overline{p^{\kappa+1}} - \overline{p}^{\kappa+1}\, d\theta, \qquad (1)$$

where the overbar denotes averaging over isentropic surfaces; $c_p$ is the specific heat capacity at constant pressure; $g$ is the gravitational acceleration; $p$ is the pressure, with $p_0$ being its mean surface value; $\kappa = R/c_p$, where $R$ is the gas constant for dry air; and $\theta$ is the potential temperature. Although Eq. (1) is exact, it is generally regarded as computationally impractical so that, in practice, a majority of APE studies have resorted to using the so-called quasigeostrophic (QG) approximation, which depends on the temperature variance on isobaric surfaces divided by static stability:

$$\overline{\mathrm{APE}_{\mathrm{Lor}}} \approx \frac{1}{2} \frac{\kappa c_p}{g p_0^{\kappa}} \int_0^{p_0} \overline{p}^{-(1-\kappa)} \left( -\frac{\partial \overline{\theta}}{\partial p} \right)^{-1} \overline{\theta'^2}\, dp, \qquad (2)$$

with the bar here denoting an average over isobaric surfaces [more detail on this derivation can be found, for example, in Grotjahn (1993)].

This definition is a common diagnostic for global characteristics of APE in climate models and observation-based data (e.g., Hu et al. 2004; Schneider and Walker 2008; O'Gorman and Schneider 2008; Hernadez-Deckers and von Storch 2010; Veiga and Ambrizzi 2013), as well as for studying the evolution of individual eddies in idealized life cycle experiments (Simmons and Hoskins 1978). However, a limitation of the quadratic approximation in Eq. (2) is that it assumes a small departure from the reference state, which may become potentially very inaccurate in areas of substantial mixing and rapidly varying static stability, such as the midlatitude storm tracks (e.g., Holliday and McIntyre 1981). Furthermore, Lorenz's definition is a global one and hence obscures regional variability and can lead to misleading results. For example, Novak et al. (2018, manuscript submitted to *J. Atmos. Sci.*) showed that meridionally confined storm tracks exhibit a spatially complex thermal equilibration, which can be translated to a local APE decrease but a global increase globally as a response to polar cooling. Such spatially complex responses cannot be captured by Lorenz's global APE definition.

So far, most attempts at seeking a local view of energetics have relied on "localizing" Lorenz APE by assuming that it is physically meaningful to study the spatial distribution of the integrand of Eq. (2) (e.g., Li et al. 2007) or Eq. (1) (e.g., Ahbe and Caldeira 2017). Although these approaches appear to yield plausible results, it goes without saying that it would be far more satisfactory to base such analyses directly from a truly local definition of APE. Other attempts of using the Lorenz energetics locally include spatial integrations over a local domain of an open system that is embedded within a closed global system (Johnson 1970). Though an exact framework, the precise spatial distribution of the various energy, conversion and transport terms is still obscure and the need for a different formulation of a local definition is apparent.

One important concept introduced as an attempt to resolve the difficulties associated with the global character of Lorenz APE is that of "exergy." In the context of atmospheric and oceanic sciences, exergy can be viewed as essentially measuring the departure of a system from its thermodynamic and mechanical equilibria. Such equilibria can be identified by defining an isothermal reference state, which was advocated by many (e.g., Dutton 1973; Pearce 1978; Blackburn 1983; Karlsson 1997). Although exergy is appealing because of its simplicity and local character, it is nevertheless fundamentally different and in general excessively larger than Lorenz APE [as stressed by Tailleux (2013a)]. This is due to the exergy depending on the system being brought to a maximum state of entropy when computing the reference state, whereas Lorenz's APE depends on the system being adiabatically rearranged while conserving entropy. It means that, in contrast to APE, the total exergy of a system includes a large chunk of the background potential energy ($\mathrm{PE}_r$), which is a "heatlike" form of potential energy and hence strongly constrained by the second law of thermodynamics.

So far, the only satisfactory approaches to construct Lorenz APE from a local principle appear to be those stemming from the two studies by Holliday and McIntyre (1981) for an incompressible fluid, and Andrews (1981) for a fully compressible stratified one-component fluid. Recently, these theories were extended to the case of a multicomponent fluid by Tailleux (2018). For all types of fluid, the authors were able to construct a locally defined positive form of potential energy density that can be interpreted as the work necessary to bring a parcel from its reference position $Z_r$ to its actual position $Z$. Thus in the case of an incompressible fluid, the APE density ($\mathrm{J\,kg^{-1}}$) takes the following simple form:

$$E_a = \frac{g}{\rho_0} \int_{Z_r}^{Z} \left[ \rho - \rho_r(Z', t) \right] dZ', \qquad (3)$$

where $\rho$ is the density and the subscript $r$ indicates the reference variables. We note that $E_a$ is positive definite and its volume integral reduces to Lorenz APE when

$\rho_r(Z, t)$ coincides with Lorenz's adiabatically sorted state of minimum potential energy (Andrews 1981). If a different kind of reference state is chosen, the volume integral of $E_a$ will in general be larger than but still comparable with Lorenz APE if $\rho_r$ is defined in terms of a horizontal or isobaric average (Tailleux 2013b). By assuming a small departure from the reference state, $E_a$ can also be reduced to the APE of small-amplitude internal waves (Holliday and McIntyre 1981): $(1/2)N^2\zeta^2$, where $N$ is the buoyancy frequency and $\zeta = Z - Z_r$ is the vertical displacement from the reference position. Note that although $E_a$ is local in the sense that it can be defined at every point of the fluid considered, it possesses some degree of nonlocality because the reference state is in general a globally defined quantity. In this respect, $E_a$ is of the same nature as most statistical quantities defined relative to some mean value, such as "anomaly" or "variance."

Aside from its local nature, other advantages of this formulation over Lorenz APE are that it is exact, valid for finite-amplitude departures from the reference position, computationally easy to implement, and definable for a wider range of reference states (such as horizontally or isobarically averaged ones, as discussed later on). For "nonsorted" reference states, the reference position of a fluid parcel is then obtained as the implicit solution of the so-called level of neutral buoyancy (LNB) equation, $\rho = \rho_r(Z_r, t)$, which holds the key to the mathematical study of the reference-state properties, even when the reference state is not explicitly known (e.g., Tailleux 2013b; Saenz et al. 2015).

Shepherd (1993) showed that the local APE density frameworks of Andrews (1981) and Holliday and McIntyre (1981) could be naturally explained in the context of Hamiltonian theory by a suitable introduction of "Casimirs." He introduced the term "pseudoenergy" to refer to the sum of kinetic energy plus APE density, allowable in principle to account for momentum constraints as well, which was later explored by Codoban and Shepherd (2003). Shepherd's pseudoenergy was in turn connected to the concept of extended exergy by Kucharski (1997) as measuring the departure from a state of mechanical equilibrium with a vertically varying temperature profile (instead of the uniform temperature $T_0$ characterizing global thermodynamic equilibrium), thus establishing the formal equivalence between the different concepts. Using this definition, Kucharski and Thorpe (2000) then presented the local distributions of the zonal-mean-based APE and conversion terms in a primitive-equation model. However, use of the exact local APE density framework for the study of atmospheric energetics has remained limited so far.

This paper aims to advocate the use of the local APE density framework in the atmosphere as a useful tool for interpreting regional dynamics. It will 1) summarize the advantages of the local framework [Eq. (3)] over the Lorenz definition [Eq. (2)] and 2) present the first three-dimensional view of the distribution and budgets of the eddy and mean APE density components in observation-based data. More specifically, section 2 introduces the precise formulation of the APE density, its mean and eddy components and their evolution equations. Section 3 uses ERA-Interim data for December–February (DJF) (Kållberg et al. 2005) to compare the Lorenz APE and its approximations to the exact locally derived APE density when globally integrated. Section 3 also reveals the three-dimensional spatial distributions and budgets of mean and eddy local APE density components, which, to the authors' knowledge, has not been shown before. Section 4 summarizes and discusses the findings and their significance to the energetics community. The following analysis is limited to the dry (one component) atmosphere, which still preserves the general features of the large-scale dynamics (Pavan et al. 1999).

## 2. Local APE density for a hydrostatic dry atmosphere

The derivation of a local principle for the APE density of a dry hydrostatic atmosphere was previously addressed by Shepherd (1993) in the context of Hamiltonian theory. His Eq. (8.1) (using his notations) for the pseudoenergy is given by

$$\mathcal{A} = \int \left( (1/2) g^{-1} |\mathbf{v}_h|^2 - \int_0^{\theta - \theta_0} c_p \{ \Pi[\mathcal{P}(\theta_0 + \hat{\theta})] - \Pi[\mathcal{P}(\theta_0)] \} \, d\hat{\theta} \right) d\mathbf{x}_h \, dp, \tag{4}$$

where $\Pi(p)$ is the Exner function, and $\mathcal{P}(\theta)$ is his notation for the reference pressure profile viewed as a function of potential temperature $\theta$.

The main aims of this section are 1) to present an alternative and arguably simpler approach that is more directly connected to the work of buoyancy forces, similar to the expressions for APE density obtained for a fully compressible nonhydrostatic fluid by Andrews (1981) and Tailleux (2018) and for Boussinesq fluids by Holliday and McIntyre (1981) and Tailleux (2013b); and 2) to show how to obtain an exact and rigorous partition of the APE density into mean and eddy components for arbitrary Reynolds averaging operators for the study of eddy–mean flow interactions, which extends and refines previous related work by Scotti and White (2014) derived in the context of the Boussinesq equations for a fluid with a linear equation of state.

*a. Construction and basic properties*

In the following, we use a pedagogical approach to construct the local APE and show its connection to the kinetic energy. To do so, we use an elementary manipulation of the horizontal momentum, hydrostatic, mass conservation, and thermodynamic equations written in the following form:

$$\frac{D\mathbf{V}}{Dt} + f\,\mathbf{k}\times\mathbf{V} + \nabla_p(\Phi-\Phi_r) = \mathbf{F}, \tag{5}$$

$$\frac{\partial(\Phi-\Phi_r)}{\partial p} = -\{\alpha(\theta,p) - \alpha[\theta_r(p,t),p]\}, \tag{6}$$

$$\nabla_p\cdot\mathbf{V} + \frac{\partial\omega}{\partial p} = 0, \tag{7}$$

$$c_p\frac{D\theta}{Dt} = \frac{\theta}{T}Q, \tag{8}$$

where $\mathbf{V} = (u, v)$ is the horizontal velocity, $\omega = Dp/Dt$ is the vertical pressure velocity, $\Phi$ is the geopotential, $f$ is the Coriolis parameter, $\mathbf{F}$ is a horizontal frictional force, and $\theta_r(p, t)$ is a time-dependent reference potential temperature profile whose computation is described in appendix A.

The equation of state for the specific volume can be written as $\alpha = RT/p = R\theta\Pi/p$, where $\Pi = (p/p_0)^{R/c_p}$ is the Exner function. For reasons that will be clarified below, it is also useful to regard the specific volume as the partial derivative of specific enthalpy $h = c_pT = c_p\Pi\theta$ at constant $\theta$; that is,

$$\alpha = \left.\frac{\partial h}{\partial p}\right|_\theta = c_p\theta\frac{\partial\Pi}{\partial p}.$$

An evolution equation for kinetic energy can be obtained in the usual way by multiplying the horizontal momentum equation [Eq. (5)] by $\mathbf{V}$, and adding it to the hydrostatic equation [Eq. (6)] multiplied by $\omega$:

$$\frac{D}{Dt}\frac{\mathbf{V}^2}{2} + \nabla_h\cdot(\Phi'\mathbf{V}) + \frac{\partial(\omega\Phi')}{\partial p} = -\{\alpha(\theta,p) - \alpha[\theta_r(p,t),p]\}\frac{Dp}{Dt} + \mathbf{F}\cdot\mathbf{V}. \tag{9}$$

The term responsible for the conversion between kinetic energy and available potential energy is the first term on the right-hand side that is proportional to $Dp/Dt$. Here, the key is to recognize that this term can be naturally expressed in terms of the total derivative of the following quantity:

$$E_a(\theta,p,t) = \int_{p_r}^{p}\{\alpha(\theta,p') - \alpha[\theta_r(p',t),p']\}\,dp', \tag{10}$$

which we will take as our definition of local APE density, where the reference pressure $p_r = p_r(\theta, t)$ is defined to satisfy the LNB equation $\{\alpha(\theta, p_r) = \alpha[\theta_r(p_r, t), p_r]\}$, similar to Tailleux (2013b). It is easy to verify that the LNB equation is equivalent to the equation $\theta_r(p_r, t) = \theta$ because of the special form of the equation of state for a perfect gas. Next, the total derivative of $E_a$ can be written as

$$\frac{DE_a}{Dt} = (\alpha-\alpha_r)\frac{Dp}{Dt} + \int_{p_r}^{p}\frac{\partial\alpha}{\partial\theta}\,dp'\frac{D\theta}{Dt} - \int_{p_r}^{p}\frac{\partial\alpha_r}{\partial t}\,dp' = \delta\alpha\omega + \Upsilon Q - \chi, \tag{11}$$

where we defined $\alpha_r = \alpha[\theta_r(p, t), t]$ for convenience. Using the fact that $\alpha = R\theta\Pi/p = c_p\theta\partial\Pi/\partial p$, it follows that we can write

$$\int_{p_r}^{p}\frac{\partial\alpha}{\partial\theta}\,dp'\frac{D\theta}{Dt} = c_p[\Pi(p) - \Pi(p_r)]\frac{D\theta}{Dt} = c_p\left(\frac{T-T_r}{\theta}\right)\frac{D\theta}{Dt} = \left(\frac{T-T_r}{T}\right)Q, \tag{12}$$

which defines the thermal efficiency $\Upsilon$ as

$$\Upsilon = \frac{\Pi(p) - \Pi(p_r)}{\Pi(p)} = 1 - [p_r(\theta,t)/p]^\kappa = \frac{T-T_r}{T}, \tag{13}$$

which is the same as was previously derived by Lorenz (1955a), and is generally denoted by $N$ in the atmospheric APE literature.

We also defined an additional diabatic term due to temporal changes in the reference state:

$$\chi = \int_{p_r}^{p}\frac{\partial\alpha_r}{\partial t}\,dp' = \int_{p_r}^{p}\frac{R\Pi(p')}{p'}\frac{\partial\theta_r}{\partial t}(p',t)\,dp'. \tag{14}$$

Note that $\chi = 0$ when the reference state is chosen to be independent of time. By combining Eqs. (11) and (9), the following evolution equation for the total mechanical energy (kinetic energy plus available potential energy) is obtained:

$$\frac{D(E_k+E_a)}{Dt} + \nabla_p\cdot(\Phi'\mathbf{V}) + \frac{\partial(\omega\Phi')}{\partial p} = \mathbf{F}\cdot\mathbf{V} + \left(\frac{T-T_r}{T}\right)Q - \int_{p_r}^{p}\frac{\partial\alpha_r}{\partial t}\,dp'. \tag{15}$$

We make the following remarks:

- Our Eq. (10) for the local APE density has a clear interpretation in terms of the work against buoyancy forces, as in Holliday and McIntyre (1981), Andrews (1981), Tailleux (2013b), and Tailleux (2018). In fact, its expression is identical to that used for estimating the convective available potential energy (CAPE) in conditionally unstable soundings (e.g., Emanuel 1994),

the only difference being the use of an arbitrary reference profile $\alpha_r(\theta, p)$ instead of one defined by a sounding;
- Eq. (10) is positive definite. Its expression in the small amplitude is most conveniently expressed by regarding the reference potential temperature profile $\theta_r$ as a function of the Exner function rather than of pressure. By using the LNB equation $[\theta = \theta_r(p_r, t)]$, it is easy to establish that

$$\begin{aligned} E_a &= \int_{p_r}^{p} c_p \frac{\partial \Pi}{\partial p}(p')\left[\theta_r(p_r,t) - \theta_r(p,t)\right] dp' \\ &= -c_p \int_{\Pi_r}^{\Pi} \int_{\Pi_r}^{\Pi'} \frac{\partial \theta_r}{\partial \Pi}(\Pi'', t)\, d\Pi''\, d\Pi' \\ &\approx -c_p \frac{\partial \theta_r}{\partial \Pi}(\Pi_r, t)\frac{(\Pi - \Pi_r)^2}{2}. \end{aligned} \tag{16}$$

  This small-amplitude limit for $E_a$ appears to be new as well and is simpler than the ones obtained previously (e.g., Shepherd 1993).
- An important feature of Eq. (11) is the presence of a nonlocal term proportional to $\partial\theta_r/\partial t$ that is absent from Lorenz global construction but can occasionally be important locally.
- As in Shepherd's (1993) expression, Eq. (10) does not require the temperature reference profile to be necessarily obtained from an adiabatic rearrangement of fluid parcels.

## Evolution of the reference temperature profile

As discussed above, the reference temperature profile is linked to the actual temperature through the LNB equation $[\theta_r(p_r, t) = \theta]$. This property can be exploited to derive an evolution equation for $\theta_r(p, t)$ in terms of the isentropic-averaged diabatic heating. Indeed, the relation implies $D\theta_r(p_r, t)/Dt = D\theta/Dt = \theta Q/T$. Expanding the latter relation yields

$$\begin{aligned} c_p \frac{D}{Dt}\theta_r(p_r,t) &= c_p\left(\frac{\partial \theta_r}{\partial t} + \omega_r \frac{\partial \theta_r}{\partial p_r}\right) \\ &= \frac{Q}{\Pi(p)} = \frac{\theta Q}{T} = \theta_r(p_r,t)\frac{Q}{T}, \end{aligned}$$

where $\omega_r = Dp_r/Dt$. It follows that by averaging on constant-$p_r$ surfaces, one obtains

$$c_p \frac{\partial \theta_r}{\partial t}(p_r,t) = \overline{Q/\Pi}^{\,p_r} = \theta\overline{\left(\frac{Q}{T}\right)}^{\,p_r},$$

where the overbar denotes averaging along a constant-$p_r$ surface, which at constant time coincides with an isentropic surface. This shows that the $\chi$ term in Eq. (14) is diabatic, and relates to the heating of the reference state.

### b. Separation into mean and eddy components

The separation of energy reservoirs into mean and eddy components traditionally relies on the introduction of a Reynolds average, denoted by an overbar, satisfying the properties for any scalar quantity $Q$: 1) $Q = \overline{Q} + Q'$, 2) $\overline{Q'} = 0$, and 3) $\overline{\overline{Q}} = \overline{Q}$. In the context of studies of the atmospheric and oceanic energy cycles, zonal averaging has been primarily used for atmospheric studies (e.g., Lorenz 1955b), whereas temporal averaging is more characteristic of oceanic studies (e.g., von Storch et al. 2012; Zemskova et al. 2015). Other important forms of averaging are the ensemble average and Lanczos filtering (although the latter does not fully satisfy the classical properties of a Reynolds average).

For a quadratic quantity such as kinetic energy, regardless the average chosen, yields a simple mean/eddy decomposition of the form $\overline{E_k} = E_k^m + E_k^e$ with $E_k^m = \overline{\mathbf{V}}^2/2$ and $E_k^e = \overline{\mathbf{V}'^2}/2$. What distinguishes APE density from kinetic energy is that it is not naturally a quadratic quantity. Thus it requires a different approach when splitting it into mean and eddy components. To that end, it is useful to introduce a nonconventional "mean" pressure $\hat{p}_r \neq \overline{p}_r$ that differs from its Reynolds average, but one that is nevertheless unaffected by the averaging operator so that $\overline{\hat{p}_r} = \hat{p}_r$. In this study, $\hat{p}_r$ is found using $\overline{\theta}_r(\hat{p}_r, t) = \overline{\theta}$ and is a function of time and the spatial coordinates (mirroring the dimensions of $\overline{\theta}$). Note here that similar ideas enter the definition of various nonstandard "mean" fields in the theory of the so-called thickness-weighted-averaged (TWA) equations (e.g., Young 2012). As a result, we can write

$$\begin{aligned} E_a = &\int_{p_r}^{\hat{p}_r} \frac{R\Pi(p')}{p'}\left[\theta - \theta_r(p',t)\right] dp' \\ &+ \int_{\hat{p}_r}^{p} \frac{R\Pi(p')}{p'}\left[\theta - \theta_r(p',t)\right] dp', \end{aligned} \tag{17}$$

so that taking the average enables the mean and eddy terms ($\overline{E_a} = E_a^m + E_a^e$) to be written as

$$E_a^m = \int_{\hat{p}_r}^{p} \left\{\alpha(\overline{\theta}, p') - \alpha\left[\overline{\theta}_r(p',t), p'\right]\right\} dp', \tag{18}$$

$$E_a^e = \overline{\int_{p_r}^{\hat{p}_r} \left\{\alpha(\theta, p') - \alpha\left[\theta_r(p',t), p'\right]\right\} dp'}. \tag{19}$$

## Evolution equations for the mean and eddy APE density

Evolution for the mean APE density is obtained by taking the material (Lagrangian) derivative of Eq. (18):

$$\frac{D_M E_a^m}{Dt} = \{\alpha(\overline{\theta},p) - \alpha[\overline{\theta}_r(p,t),t]\}\,\overline{\omega} + \int_{\hat{p}_r}^{p} c_p \frac{\partial \Pi}{\partial p}(p')\,dp' \frac{D_M \overline{\theta}}{Dt} - c_p \int_{\hat{p}_r}^{p} \frac{\partial \Pi}{\partial p}(p') \frac{\partial \overline{\theta}_r}{\partial t}\,dp'$$

$$= \{\alpha(\overline{\theta},p) - \alpha[\overline{\theta}_r(p,t),t]\}\overline{\omega} + c_p[\Pi(p) - \Pi(\hat{p}_r)] \frac{D_M \overline{\theta}}{Dt} - c_p \int_{\hat{p}_r}^{p} \frac{\partial \Pi}{\partial p}(p') \frac{\partial \overline{\theta}_r}{\partial t}\,dp', \tag{20}$$

where

$$\frac{D_M}{Dt} = \frac{\partial}{\partial t} + \overline{u}\frac{\partial}{\partial x} + \overline{v}\frac{\partial}{\partial y} + \overline{\omega}\frac{\partial}{\partial p} \tag{21}$$

denotes the tendency plus advection by the mean flow. The above equations depend on the Reynolds-averaged thermodynamic equation for potential temperature, which is easily shown to be

$$\frac{D_M \overline{\theta}}{Dt} = -\nabla \cdot \overline{\mathbf{v}'\theta'} - \frac{\partial \overline{\omega'\theta'}}{\partial p} + \frac{\overline{\theta}}{\overline{T}} \frac{\overline{Q}}{c_p}. \tag{22}$$

Note that the latter equation exploits the very special property that $\Pi(p) = \overline{T}/\overline{\theta} = T/\theta$. We can also define a mean reference temperature as $\hat{T}_r = \Pi(\hat{p}_r)\overline{\theta}$, which is not a Reynolds average, and is hence denoted by a hat. We can define a mean thermodynamic efficiency as the following equivalent mathematical relations:

$$\hat{\Upsilon} = \frac{\overline{T} - \hat{T}_r}{\overline{T}} = 1 - \frac{\Pi(\hat{p}_r)}{\Pi(p)} = \frac{p^\kappa - \hat{p}_r^\kappa}{p^\kappa}. \tag{23}$$

The second term in Eq. (20) can therefore be rewritten as

$$c_p[\Pi(p) - \Pi(\hat{p}_r)] \frac{D_M \overline{\theta}}{Dt} = \hat{\Upsilon}\overline{Q} - \nabla \cdot \left[\Pi(p) - \Pi(\hat{p}_r)\overline{\mathbf{u}'\theta'}\right] + \overline{\mathbf{u}'\theta'} \cdot \nabla[\Pi(p) - \Pi(\hat{p}_r)],$$

where the quantity $\Pi(p) - \Pi(\hat{p}_r) = \hat{\Upsilon}\overline{T}/\overline{\theta}$. The evolution equation for the mean APE density can therefore be written in the form

$$\frac{\partial E_a^m}{\partial t} = \underbrace{-\overline{\mathbf{u}} \cdot \nabla E_a^m}_{\text{Advection}} + \underbrace{\overline{\delta\alpha}\,\overline{\omega}}_{C[E_k^m \to E_a^m]} - \underbrace{c_p \nabla \cdot \left(\overline{\mathbf{u}'\theta'}\,\frac{\overline{T}\hat{\Upsilon}}{\overline{\theta}}\right) + c_p \overline{\mathbf{u}'\theta'} \cdot \nabla\left(\frac{\overline{T}\hat{\Upsilon}}{\overline{\theta}}\right)}_{C[E_a^m \to E_a^e]} \underbrace{-\hat{\chi} + \hat{\Upsilon}\overline{Q}}_{\text{Diabatic}}, \tag{24}$$

where

$$\hat{\chi} = \int_{\hat{p}_r}^{p} \frac{\partial \Pi}{\partial p}(p') \frac{\partial \overline{\theta}_r}{\partial t}\,dp'. \tag{25}$$

Note that again $\hat{\chi} = 0$ when the reference state is chosen to be independent of time. The physical interpretation of the terms on the RHS of Eq. (24) is indicated. Namely, these terms are mean advection of the mean APE, conversion between the mean APE and mean kinetic energy ($C[E_k^m \to E_a^m]$), conversion between the mean APE and eddy APE ($C[E_a^m \to E_a^e]$), and a diabatic heating term. The $C[E_k^m \to E_a^m]$ conversion is equivalent to that of the QG Lorenz definition. The first of the $C[E_a^m \to E_a^e]$ terms vanishes under global integration. The second term of the conversion is similar to the QG Lorenz conversion, though it includes an additional component that becomes important under large static stability, as is demonstrated below:

$$C[E_a^m \to E_a^e]_2 = c_p \overline{\mathbf{u}'\theta'} \cdot \nabla\left(\frac{\overline{T}}{\overline{\theta}}\hat{\Upsilon}\right) = c_p \overline{\mathbf{u}'\theta'} \cdot \nabla[\Pi(p) - \Pi(\hat{p}_r)].$$

To that end, note that from the defining relation of $\hat{p}_r$, namely $\overline{\theta}_r(\hat{p}_r, t) = \overline{\theta}$, we can write

$$\frac{\partial \overline{\theta}_r}{\partial p}\nabla \hat{p}_r = \nabla\overline{\theta}.$$

As a result, the $C[E_a^m \to E_a^e]_2$ conversion term becomes

$$C[E_a^m \to E_a^e]_2 = c_p\left[\frac{\partial \Pi}{\partial p}(p)\overline{\omega'\theta'} - \frac{\partial \Pi}{\partial p}(\hat{p}_r)\left(\frac{\partial \overline{\theta}_r}{\partial p}\right)^{-1} \overline{\mathbf{u}'\theta'} \cdot \nabla\overline{\theta}\right]$$

$$= \frac{R}{p_0^\kappa}\left[p^{\kappa-1} - \hat{p}_r^{\kappa-1}\left(\frac{\partial \overline{\theta}_r}{\partial p}\right)^{-1}\frac{\partial \overline{\theta}}{\partial p}\right]\overline{\omega'\theta'} - \frac{R\hat{p}_r^{\kappa-1}}{p_0^\kappa}\left(\frac{\partial \overline{\theta}_r}{\partial p}\right)^{-1} \overline{\mathbf{v}'\theta'} \cdot \nabla_p\overline{\theta}$$

$$= \frac{R}{p_0^\kappa}\left[p^{\kappa-1} - \hat{p}_r^{\kappa-1}\frac{\partial \hat{p}_r}{\partial p}\right]\overline{\omega'\theta'} - \frac{R\hat{p}_r^{\kappa-1}}{p_0^\kappa}\left(\frac{\partial \overline{\theta}_r}{\partial p}\right)^{-1} \overline{\mathbf{v}'\theta'} \cdot \nabla_p\overline{\theta}.$$

This term is dominated by the second term that involves the isobaric gradient of the mean temperature $\nabla_p\overline{\theta}$. The case where mean APE is converted to eddy APE corresponds to the case where $C[E_a^m \to E_a^e]_2 < 0$. This

corresponds to the case where $\overline{\mathbf{v}'\theta'} = -K_e \nabla_p \overline{\theta}$ is downgradient, in which case,

$$C\left[E_a^m \to E_a^e\right]_2 \approx K_e \frac{R\hat{p}_r^{\kappa-1}}{p_0^{\kappa}} \left(\frac{\partial \overline{\theta}_r}{\partial p}\right)^{-1} \left|\nabla_p \overline{\theta}\right|^2 < 0.$$

The resulting expression is somewhat different from the classical Lorenz expression, in that there is now a contribution from the vertical heat flux in the expression, which is small for a stable stratification but can become large when static stability of the mean profile $\partial\overline{\theta}/\partial p > 0$, which avoids the cancellation. This new term was previously noted by Zemskova et al. (2015) and is one of the novelties offered by the finite-amplitude framework.

We now turn to the derivation of an evolution equation for the eddy APE density. This is obtained by subtracting the evolution equation of the mean APE density from the mean of the total APE density equation:

$$\frac{D_M E_a^e}{Dt} = \frac{D_M \overline{E}_a}{Dt} - \frac{D_M E_a^m}{Dt}, \tag{26}$$

where

$$\frac{D_M \overline{E}_a}{Dt} = \overline{\frac{DE_a}{Dt}} - \overline{\mathbf{u}' \cdot \nabla E_a'}. \tag{27}$$

Given that we can write the evolution equation for the total APE density as

$$\frac{DE_a}{Dt} = \delta\alpha\omega + \Upsilon Q - \chi, \tag{28}$$

it follows that the mean is given by

$$\begin{aligned}\overline{\frac{DE_a}{Dt}} &= \overline{\delta\alpha}\,\overline{\omega} + \overline{\delta\alpha'\omega'} + \overline{\Upsilon}\,\overline{Q} + \overline{\Upsilon'Q'} - \overline{\chi} \\ &= \frac{D_M \overline{E}_a}{Dt} + \nabla \cdot \left(\overline{\mathbf{u}' E_a'}\right),\end{aligned}$$

which implies

$$\begin{aligned}\frac{D_M (E_a^m + E_a^e)}{Dt} = {} & \overline{\delta\alpha}\,\overline{\omega} + \overline{\delta\alpha'\omega'} + \overline{\Upsilon}\,\overline{Q} \\ & + \overline{\Upsilon'Q'} - \overline{\chi} - \nabla \cdot \left(\overline{\mathbf{u}' E_a'}\right).\end{aligned} \tag{29}$$

Note that we have

$$\delta\alpha = c_p \frac{\partial \Pi}{\partial p}(p)\left[\theta - \theta_r(p,t)\right],$$

hence

$$\overline{\delta\alpha} = c_p \frac{\partial \Pi}{\partial p}(p)\left[\overline{\theta} - \overline{\theta}_r(p,t)\right].$$

A difficulty arises with the partitioning of the thermal efficiency into mean and eddy components. Indeed, the thermal efficiency is defined by

$$\Upsilon = \frac{\Pi(p) - \Pi(p_r)}{\Pi(p)}.$$

However, because

$$\overline{\Pi(p_r)} \neq \Pi(\hat{p}_r),$$

subtracting the equation for the mean APE density yields

$$\begin{aligned}\frac{\partial E_a^e}{\partial t} = {} & \underbrace{-\overline{\mathbf{u}} \cdot \nabla(E_a^e)}_{\text{Mean advection}} - \underbrace{\nabla \cdot \left(\overline{\mathbf{u}' E_a'}\right)}_{\text{Eddy advection}} + \underbrace{\overline{\delta\alpha'\omega'}}_{C\left[E_k^e \to E_a^e\right]} \\ & + \underbrace{c_p \nabla \cdot \left(\overline{\mathbf{u}'\theta'}\,\frac{\overline{T}\hat{\Upsilon}}{\overline{\theta}}\right) - c_p \overline{\mathbf{u}'\theta'} \cdot \nabla\left(\frac{\overline{T}\,\overline{\Upsilon}}{\overline{\theta}}\right)}_{C[E_a^m \to E_a^e]} \\ & + \underbrace{\overline{\Upsilon'Q'} + (\overline{\Upsilon} - \hat{\Upsilon})\overline{Q} + \hat{\chi} - \overline{\chi}}_{\text{Diabatic}}.\end{aligned} \tag{30}$$

The nature of the terms is again indicated. In particular we have the mean advection of the eddy APE, eddy advection of the total APE, conversion between the eddy APE and eddy KE ($C[E_a^e \to E_k^e]$; equivalent in the Lorenz formulation), the $C[E_a^m \to E_a^e]$ conversion, and diabatic terms due to the parcel heating and due to the environmental heating. Note the presence of additional small terms that arise from the difference between the nonconventional mean and standard Reynolds mean of some variables.

## 3. Basic illustrations

The main aim of this section is to illustrate the usefulness of the local APE framework. The first part focuses on the comparison between the local APE framework and the classical APE formulations proposed by Lorenz (1955b), in order to demonstrate their equivalence and that the (globally integrated) local APE density provides more accurate estimates of the global APE than the commonly used QG Lorenz approximation. Then, we present the three-dimensional view of the local APE density, its eddy and mean components, and the components' budgets. This will reveal the zonally asymmetric distribution of the APE components as well as its usefulness in studying the spatiotemporal variability of the atmospheric circulation.

### a. Global values and connection to Lorenz APE

This section compares the globally integrated local APE density to the exact Lorenz APE [Eq. (1)] and its QG approximations [Eq. (2)]. Two datasets from the ERA-Interim (Kållberg et al. 2005) archive were used, one with isobaric and one with isentropic vertical coordinates, both 6 hourly and spanning the years 1979–2016. For illustrative purposes, only data from 1 January of each year were selected; therefore, these sets of data samples are independent in time on daily to seasonal time scales. The reference state of the local APE density was calculated by adiabatically rearranging parcels in an ascending order, that is, by sorting all parcels based on their potential temperature using the "quicksort" algorithm at each time step. This makes the reference state equivalent to the reference state of Lorenz APE, so theoretically the exact Lorenz APE should equal to the globally integrated local APE density (Andrews 1981). For comparison, local APE calculated using a reference state that is an average potential temperature on isobaric surfaces is also displayed (see appendix A for more detail). Computing the Lorenz APE is somewhat more efficient. On a standard personal computer, 20 time steps took 6 s or less for the Lorenz APE diagnostics, 25 s for the local APE density using the isobaric $\theta_r$, and 2 min for the local APE density using the quicksort $\theta_r$.

Figure 1 shows that the local APE on isobaric surfaces is slightly lower than the exact Lorenz APE evaluated on isentropic surfaces. Because the minimum and maximum values of the isobaric and isentropic surfaces do not exactly match the maximum and minimum values of the variable pressure and potential temperature in the respective reanalysis datasets, an exact match between the isobarically based local APE and isentropically based exact Lorenz APE is not necessarily expected. Nevertheless, the local APE is the closest match to the exact Lorenz APE, better than the QG Lorenz approximation on isentropic surfaces and substantially better than the QG Lorenz approximation on isobaric surfaces (the latter being the most commonly used diagnostic for the APE).

The QG approximation of Lorenz APE is often studied with respect to the Lorenz cycle, where both kinetic energy and QG APE on pressure surfaces are split into their mean and eddy components. The four resulting evolution equations (one for each $E_a^m$, $E_k^m$, $E_a^e$, and $E_k^e$) form a closed system in the absence of diabatic and frictional processes, which makes the system (referred to as the Lorenz cycle) an attractive theory for studying energy exchanges.

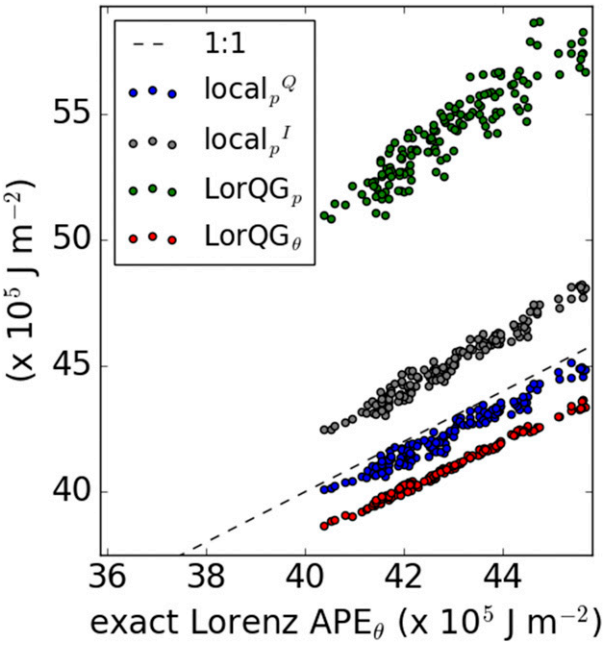


FIG. 1. Globally integrated local APE (blue: calculated using the quicksort $\theta_r$; gray: calculated using the isobarically averaged $\theta_r$) compared to the exact Lorenz APE on isentropic surfaces ($x$ axis), and the QG Lorenz approximations on isentropic (red) and isobaric (green) surfaces. The dashed line is the 1:1 line. The data are from 1 Jan (four time steps 6 h apart) of years 1979–2016 in ERA-Interim.

It is apparent from Eqs. (24) and (30) that the local eddy and mean APE density equations can be used with the mean and eddy kinetic energy equations (both of which are already of a local nature) in order to obtain a local and exact version of the Lorenz cycle (i.e., a system of the four evolution equations that is closed under adiabatic conditions). When globally integrated the two energy cycles are equivalent, apart from small differences in formulation of three terms: mean APE, eddy APE, and the $C[E_a^m \rightarrow E_a^e]$ conversion. These three terms are compared for the QG Lorenz and globally integrated local frameworks in Fig. 2.

Both eddy and mean APE components are overestimated by the QG approximation, corresponding to the total APE being larger. The conversion term is of a similar magnitude with some spread, resulting from the QG approximation being less accurate under large static stability. However, we have found there is no simple linear relationship between static stability and the difference between the two conversions.

### b. Spatial distribution and variance of APE components

This section focuses on the three-dimensional structure of the eddy and mean APE density components and

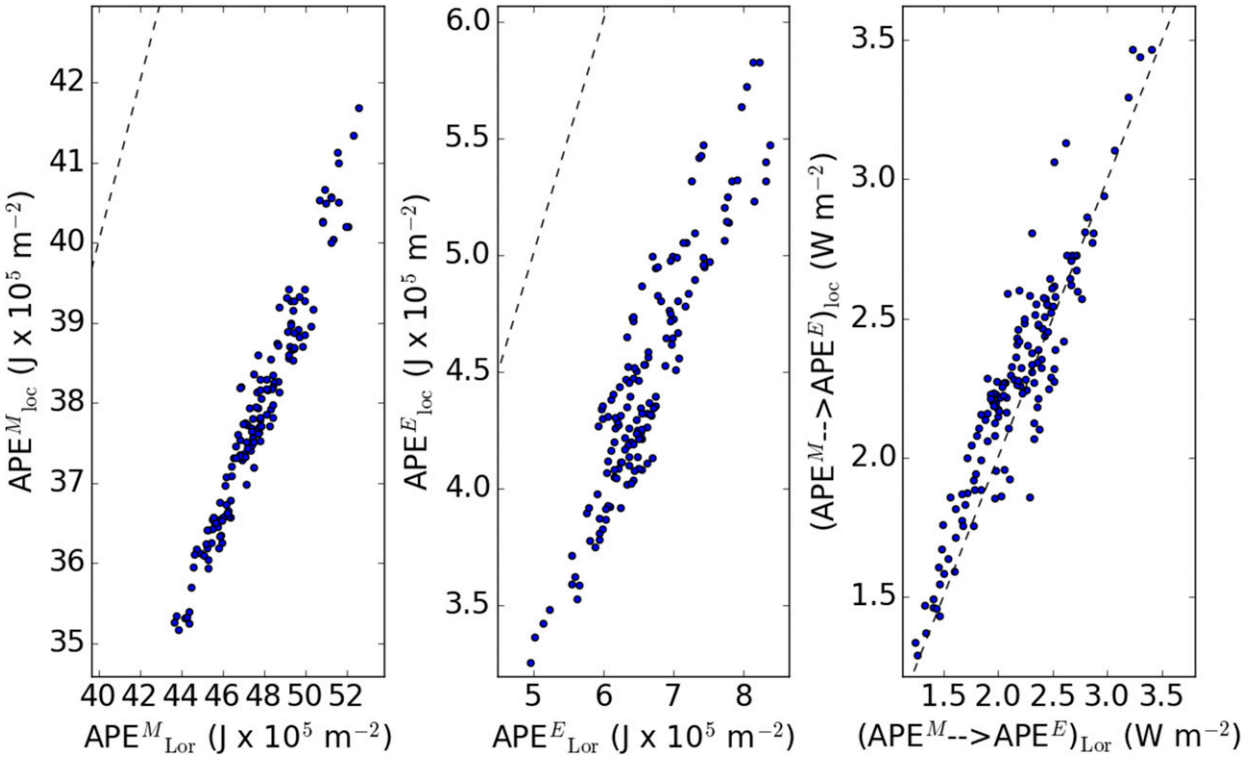


FIG. 2. Lorenz QG APE compared to the globally integrated local APE, with both being evaluated on isentropic surfaces and split into their (left) mean and (center) eddy components. (right) The conversion between the mean and eddy APEs for the two frameworks is also shown. The dashed line is the 1:1 line. The data are from 1 Jan (four time steps 6 h apart) of years 1979–2016 in ERA-Interim.

their interannual variability. We focus on the winters (DJF) of years 1979–2016 in daily averaged ERA-Interim data. The winter season was selected because during winter the midlatitudes are dominated by strong eddies that are particularly interactive with the mean large-scale circulation, and this interaction will be the focus of a forthcoming paper.

For the same reason, we separate the APE density into eddy and mean components using the 10-day Lanczos filter (Duchon 1979). This way the eddy component mainly corresponds to high-frequency baroclinic transients that are associated with synoptic storms, and the mean component corresponds to more slowly varying circulations, such as the midlatitude jet (Hoskins et al. 1983; Novak et al. 2015). Another (more technical) advantage of this separation is that it also allows investigation of APE in all three spatial dimensions (rather than only two dimensions when the zonal mean is used for the separation), as well as in time (which would not be possible had the time mean been used). Comparison between the two separation methods (i.e., using the zonal mean versus the Lanczos filter) is shown in appendix B.

We also use the isobaric average (instead of the quicksort method) to compute the reference potential temperature profile, because it avoids extremely high APE density values at the surface due to extremely high (and potentially badly constrained) potential temperature values from the top of the atmosphere (see appendix A).

The three-dimensional spatial distribution of the eddy and mean APE density is displayed in Fig. 3, along with their interannual standard deviations (i.e., based on the departures of annual values from the long-term mean of all winters). The mean APE density (top row; J m$^{-2}$) is most concentrated in the upper levels of high latitudes and exhibits a minimum in the midlatitudes with a secondary maximum in the tropics. This zonally averaged profile is expected because 1) it has been shown before (Kucharski 1997; Kucharski and Thorpe 2000), and 2) by definition (since $\theta$ on average decreases continuously with latitude) the high and low latitudes are characterized by the largest departures from the globally horizontally constant reference state (and the high latitudes are more extreme because they cover a smaller surface area). Similarly, eddy APE density distribution (bottom row) is as expected, peaking near the upper levels of the midlatitudes and mirroring the eddy KE (e.g., Kucharski and Thorpe 2000).

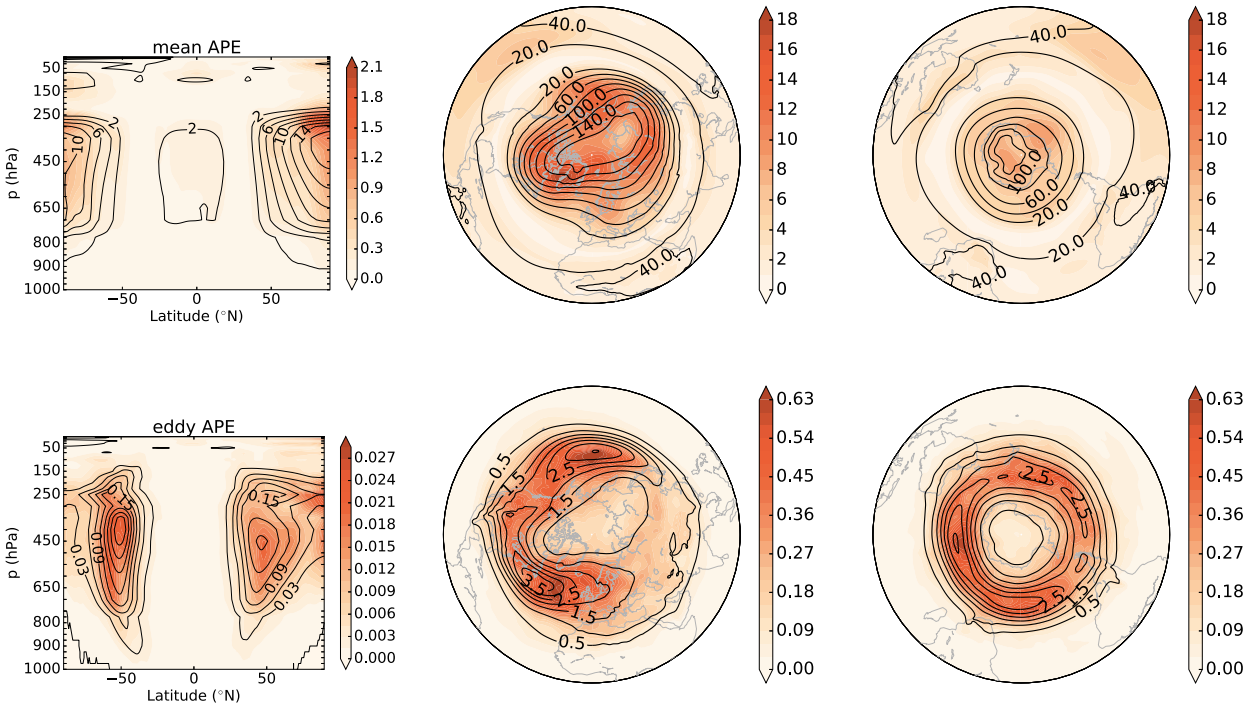


FIG. 3. (top) Mean and (bottom) eddy APE distributions (black contours), (left) zonally averaged, and vertically integrated (using mass weighting) of the (center) Northern and (right) Southern Hemispheres. The shading refers to the annual standard deviation. The split into mean and eddy components is based on the Lanczos filter, and the units are scaled to be $10^5\,\mathrm{J\,m^{-2}}$.

The zonal asymmetries of the APE density components are such that the mean APE density follows the general structure of the mean temperature and PV fields (not shown) with maxima extending more equatorward over continents. This is especially apparent in the Northern Hemisphere. Downstream of these regions of enhanced mean APE density are maxima in eddy APE density, which peak over the main storm-track regions over the North Atlantic, the North Pacific, and the Southern Oceans (e.g., Kaspi and Schneider 2013). In a thought experiment where the atmosphere could be brought to a state of zero baroclinicity (i.e., no meridional temperature gradients), the mean APE density maxima can be seen as energy reservoirs that fuel the midlatitude storm tracks between them (as is shown more explicitly in the next section).

The standard deviations of the mean and eddy APE density components are shown in colors in Fig. 3. The highest interannual variability in the mean APE density of the Northern Hemisphere is above Greenland, with secondary maxima in the North Pacific and over central northern Siberia. The Southern Hemisphere in DJF exhibits a dipole centered over the South Pole, with the stronger maximum being above the Ross Sea. Some enhanced variability is also apparent in the tropical central Pacific, where ENSO operates. The variability of the eddy APE density is generally most pronounced near the central and end parts of the storm tracks.

### c. *Thermal efficiency*

It is of interest to investigate the thermal efficiency defined in Eq. (23), because it is the factor that determines the sign and magnitude of the effect of 1) diabatic heating on the APE generation and dissipation and 2) the APE conversion into eddy energy. This efficiency is identical to that discussed by Lorenz (1955a) and several other authors (e.g., Siegmund 1994), and its magnitude and distribution, as shown in Fig. 4, is comparable to the previously published estimates. However, here we additionally show the full horizontal structure, as well as the interannual variability.

Since the thermal efficiency is defined as the departure of the actual thermal state from a reference state, it is apparent that the QG Lorenz assumption of this being of small amplitude is a poor one. The QG Lorenz APE and $C[E_a^m \rightarrow E_a^e]$ terms are defined using the thermal efficiency. It is therefore unsurprising that these terms are of a somewhat different magnitude, as shown in the previous sections.

The thermal efficiency also displays high annual variability, as shown by the standard deviation in colors. The most variable regions are in the northwestern

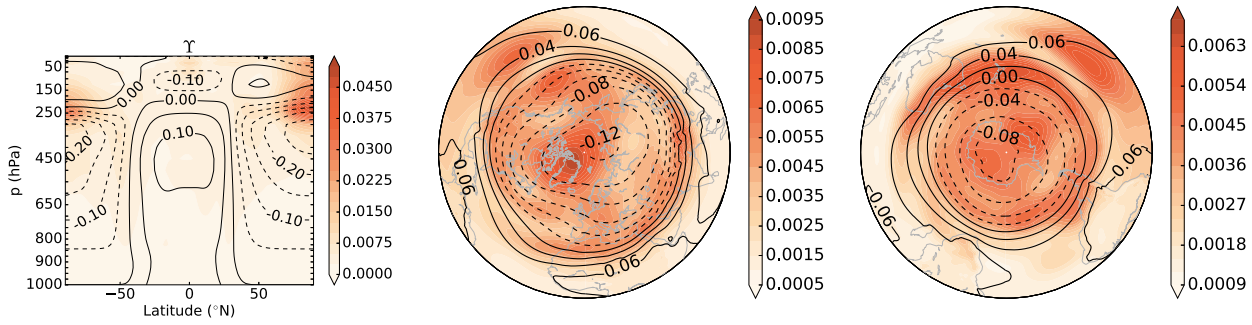


FIG. 4. Thermal efficiency ϒ (black contours), (left) zonally averaged, and horizontally averaged (using mass weighting) of the (center) Northern and (right) Southern Hemispheres. The shading refers to the annual standard deviation. The efficiency is dimensionless.

Pacific, over Greenland, and near the coast of West Antarctica. A cross-hemispheric wave train–like pattern emerges in the central Pacific. Some of these features mimic those of the mean APE density variability, and are relevant for climate sensitivity studies.

### d. *Mean and eddy local APE density budgets*

The mean and eddy local APE density budgets [i.e., terms in Eqs. (24) and (30)] are plotted for both hemispheres in Figs. 5 and 6, respectively. The sum of the diabatic terms is calculated as a residual of the nondiabatic terms in the two evolution equations. Again, we use the 10-day Lanczos filter to separate into mean and eddy terms, but this separation produces a small leakage because of the noncommutability of the mean (i.e., $\overline{X} \neq \overline{\overline{X}}$ if the overbar represents a mean derived from the Lanczos filter). This leakage is included in the residual diabatic terms. However, its magnitude was found to be small and the associated eddy and mean heating rates are comparable to those derived in previous works using different methods (e.g., Kållberg et al. 2005). Note that the conversion term ($C[E_a^m \rightarrow E_a^e]$) is not displayed in Fig. 6 of the eddy APE density budget, because it is already shown in Fig. 5 (only the sign would change in the eddy APE density equation). The conversion and heating terms were checked against existing estimates (Oort 1964; Kållberg et al. 2005; Li et al. 2007) to ensure that the obtained values are plausible.

Turning to the first terms in both budgets, the respective tendencies of the mean and eddy APE densities are nonzero, even though they are averaged over time. The reader is reminded that these averages are limited to the winter season, so the nonzero values represent changes throughout that season. Though small, these changes are such that both APE density components increase in the Northern Hemisphere and decrease in the Southern Hemisphere throughout the season.

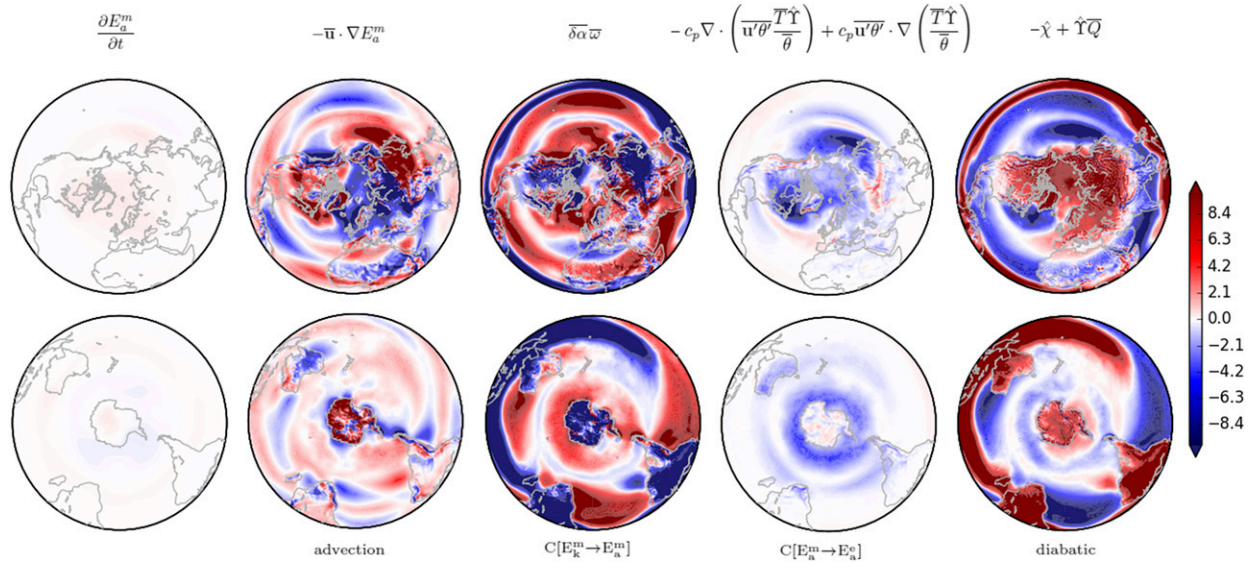


FIG. 5. Local mean APE budget [W m$^{-2}$; Eq. (24)] for the (top) Northern and (bottom) Southern Hemispheres. All terms are vertically integrated.

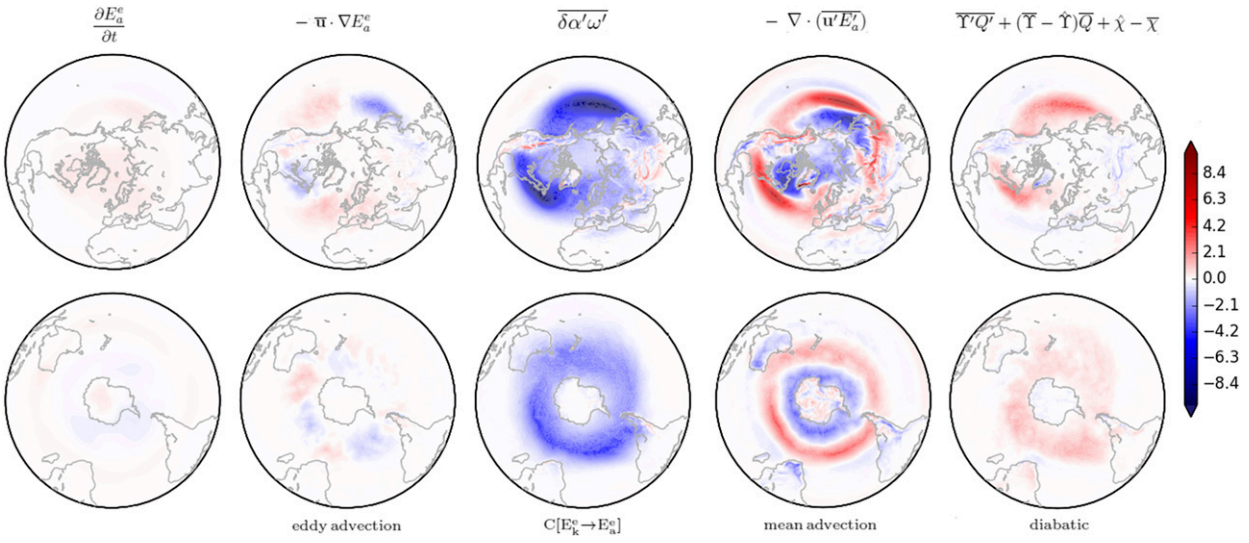


FIG. 6. Local eddy APE budget [W m$^{-2}$; Eq. (30)] for the (top) Northern and (bottom) Southern Hemispheres. All terms are vertically integrated.

The mean APE density budget is dominated by the $C[E_k^m \rightarrow E_a^m]$ conversion and the diabatic generation of the mean APE density. The diabatic term is almost entirely dominated by the $\overline{\Upsilon}\,\overline{Q}$ component (not shown), which itself follows observed diabatic heating and cooling rates (e.g., Kållberg et al. 2005). More specifically, the tropics are the main diabatic generation regions of mean APE density, though there is a secondary maximum over the poles, corresponding to the large observed radiative heating and cooling rates in those regions. Both tropical heating and polar cooling increase the large-scale meridional temperature gradients, and thus the local departures from the global reference state, that is, the mean APE density. On the other hand, diabatic mean APE density dissipation corresponds to these large-scale temperature gradients being reduced. This happens in the subtropics where cooling occurs over the return flow of the oceanic subtropical gyres, and within the midlatitude storm tracks where (mostly) latent heating reduces the large-scale temperature gradients (Hoskins and Valdes 1990; Kållberg et al. 2005).

A large part of the diabatic contributions is compensated for by the $C[E_k^m \rightarrow E_a^m]$ conversion, especially in the tropics. This term is relatively weak in the midlatitudes because the circulation there is dominated by eddy motions, and the dipole in the central Pacific mirrors the change in sign of the vertical motion of the Walker circulation.

This conversion is often interpreted as representing the mean overturning circulation (James 1994). However, one needs to consider that this term is defined with relation to the global reference state in this study (as it is in the Lorenz framework). For example, at the poleward edge of the Hadley cell the buoyancy difference [equivalent to $\overline{\delta\alpha}$ in Eq. (24)] with respect to the global reference state is positive, but the difference with respect to the immediate surroundings is negative (as is the case for parcels in thermally direct circulations, such as the Hadley cell). Since this region is characterized by descending motion (positive $\omega$), the $C[E_k^m \rightarrow E_a^m]$ conversion in this region is positive, whereas it would be negative for a more local reference state. This demonstrates the importance of choosing the correct reference state for the study of interest. In this and Lorenz's case, the sign of the $C[E_k^m \rightarrow E_a^m]$ conversion does not reflect the sign of the overturning circulation. Rather, it indicates how the local vertical motions contribute to the large-scale baroclinicity. The freedom to choose a reference state that is appropriate for the study of interest is only possible with the local framework, but not the Lorenz framework.

The mean APE density is converted into eddies ($C[E_a^m \rightarrow E_a^e]$) predominantly poleward of all storm tracks, with some weak conversions on their equatorward side. This is despite the predominant diabatic generation of APE density being in the tropics, suggesting that eddies preferably tap into the APE reservoir poleward of the storm track. The mean advection of the mean APE density is the only term that is positive at the beginning of storm tracks, indicating that advection is crucial for supplying the mean APE density to fuel storm tracks.

Moving on to the eddy APE density budget, it is apparent that conversions from mean APE ($C[E_a^m \rightarrow E_a^e]$) and into eddy kinetic energy ($C[E_a^e \rightarrow E_k^e]$) are the dominant terms, in agreement with observations of preferred

energy flows of global energy [e.g., analysis of the Lorenz cycle in Oort (1964)]: $E_a^m \rightarrow E_a^e \rightarrow E_k^e (\rightarrow \text{Friction})$. The $C[E_a^m \rightarrow E_a^e]$ and $C[E_a^e \rightarrow E_k^e]$ conversions are located poleward of and at the location of the storm tracks, respectively.

As for the remaining terms, eddies advect the total APE density to the equatorward flank of the storm tracks. A small amount of eddy APE density is advected by the mean flow farther downstream of the storm tracks, and a small amount is generated by sensible and latent heating from preexisting eddies within the storm tracks (since the largest contributor is the $\overline{\Upsilon' Q'}$ component).

In summary, it is evident that the classical Lorenz cycle of global energy flows is more complicated regionally. In particular, the conversion between the mean energies ($C[E_k^m \rightarrow E_a^m]$) is the dominant term regionally, though it is near zero if integrated globally. It is evident that energy advection into the midlatitudes is essential for fueling the storm tracks and that this energy is mainly supplied from high latitudes, perhaps because that is where the mean APE density has to be more concentrated than in the tropics because of the spherical geometry.

## 4. Discussion and conclusions

In this paper, we have developed and extended Holliday and McIntyre's (1981) and Andrews's (1981) local APE density theory to the case of a dry hydrostatic atmosphere, and illustrated its usefulness using ERA interim data. The main new advances are 1) a simpler mathematical expression for the APE density that is physically more revealing than that previously derived, 2) accounting for diabatic effects, 3) an exact separation between mean and eddy components valid for any form of Reynolds averaging, and 4) a demonstration of the feasibility of defining reference position for fluid parcels even for nonsorted reference states. Because this formulation has seldom been used on diagnostic studies, we advocate its use by presenting its new form on isobaric coordinates, by comparing it to the classical global definition suggested by Lorenz (1955b), and by presenting an illustration of its usefulness for understanding the spatiotemporal variability of the large-scale circulation.

Although the Lorenz APE definition is by far the most commonly used measure of the observed APE, we have found the following advantages if the local APE density is used instead:

- *Computational feasibility versus accuracy:* Lorenz's exact APE definition is based on averaging on isentropic surfaces, but datasets are rarely available in isentropic coordinates. Additionally, Lorenz APE is the difference between two large terms (the potential energy of an actual state and that of a reference state), which makes the calculations highly sensitive to small numerical errors. The Lorenz APE is therefore most commonly diagnosed as its QG approximation on isobaric surfaces, but this easily computable approximation comes at the cost of accuracy. On the other hand, one does not have to compromise with the local APE density, which is both exact for finite-amplitude departures from Lorenz reference state and easily computable from isobarically based data. Additionally, the globally integrated local APE density is a sum of small positive-definite values (instead of a difference between two large terms), which is always preferable from the computational viewpoint. Although the computation time of the local APE density is four times as large as that for the Lorenz diagnostics (though the exact computation time depends on the method to calculate $\theta_r$), this remains manageable and seems a small price to pay in view of the considerably greater accuracy achieved.
- *Energy conservation:* It is important to note that the hydrostatic primitive equations conserve the quantity $\mathbf{V}^2/2 + h$ rather than the full energy $\mathbf{U}^2/2 + gz + e$, where $\mathbf{U}$ is the full velocity field while $\mathbf{V}$ is its isobaric component. As for the respective forms of potential energy, only their volume-integrated values are comparable, since specific enthalpy $h$ differs from $gz + e$ at all points of the fluid. Indeed, it is well known that for a hydrostatic atmosphere, the volume integrals of each quantity are equal up to a boundary term that vanishes in absence of orography, namely,

$$\int_V (gz + e)\, dm = \int_V h\, dm + \text{Boundary term}. \quad (31)$$

The differences in energy conservation principles satisfied by the hydrostatic primitive and full Navier–Stokes equations are important, because they are necessary to realize that Lorenz definition of APE relies on the "true" form of potential energy, whereas local APE theory builds upon the particular form of energy conservation relevant to the particular system of equations considered. As a result, the volume integral of the APE density

$$\int_V E_a\, dm = \int_V (h - h_r)\, dm + \int_V \left[\Phi_r(p) - \Phi_r(p_r)\right] dm, \quad (32)$$

is not necessarily equal to Lorenz APE in presence of orography, as the latter generally causes the last term

on the right-hand side of Eq. (32) to be nonzero in general.

- *Local diagnosis:* Some studies use the Lorenz QG approximation locally, which gives physically plausible results (e.g., Li et al. 2007). However, the Lorenz APE definition formally relies on the APE being defined as a global integral. This is not the case for the local APE density, which can be formally and exactly defined locally. In combination with the kinetic eddy and mean energies (which are already of a local nature), the local APE can also be used to derive a local version of the Lorenz energy cycle.
- *Local reference state:* As opposed to the Lorenz definition, which requires the reference state to be an adiabatic rearrangement of the actual global state, the local APE framework accommodates other reference states that can be locally defined (much like buoyancy).

As predicted theoretically, using reanalysis data we confirmed that the globally integrated local APE density is more comparable to the exact Lorenz definition than the QG Lorenz approximation. A rather surprising discrepancy was found between the QG APE computed on isentropic surfaces and the QG APE computed on isobaric surfaces, which are often assumed to be closely related (Lorenz 1955b).

We also demonstrated how the mean and eddy components of APE vary both in space and in time in 35 DJF seasons in both hemispheres, so both the winter and summer seasons were studied. We used the 10-day Lanczos filter to separate the APE density into its eddy and mean components, so that eddy quantities had the characteristics of synoptic-scale eddies. Although we were not restricted to using the global state to define the local APE density, we chose to do so in order to stay in the context of the existing literature. We defined the global reference state as the isobaric average of potential temperature. The disadvantage of using a global reference state is that (as in the Lorenz definition) the atmosphere is assumed to be capable of equilibrating itself to a state of zero baroclinicity, which is clearly not something that is observed. Nevertheless, insightful results can be obtained, as long as the dependency of the APE on its reference state is considered with care.

The local APE density calculated here represents temperature deviations from the global isentropic average, so the APE density is especially abundant over the poles and the tropics, as shown before by Kucharski (1997) and Kucharski and Thorpe (2000). As far as we are aware, the zonally asymmetric APE density distribution is shown here for the first time, and it is particularly zonally asymmetric in the Northern Hemisphere, following a similar structure to the large-scale mean temperature or potential vorticity. The local APE density should not be seen as the growth rate for baroclinic eddies, which depends on the meridional temperature gradients (Eady 1949; Pedlosky 1992) rather than the departures from the isobaric mean. The eddy growth rate is maximum at the latitude of storm tracks (e.g., Hoskins and Valdes 1990), whereas APE density is maximum in the polar and tropical regions.

Nevertheless, the budgets and the interannual variabilities of the mean and eddy APE density components provide useful insights on baroclinic eddy growth and other aspects of the large-scale dynamics. For example, the illustrations within this study show the following:

- The classical studies of baroclinic eddy life cycles (e.g., Simmons and Hoskins 1978) have shown that the primary energy exchanges, as diagnosed by the Lorenz framework, are.

$$\text{Diabatic processes} \rightarrow E_a^m \rightarrow E_a^e \rightarrow E_k^e (\rightarrow \text{Friction}).$$

  This energy pathway is also observed for global time-mean observations of the atmosphere (e.g., Oort 1964), indicating that the global energetics are primarily governed by baroclinic instability. While this pathway also seems to exist locally within the storm tracks, it is apparent that the conversion between the mean energies often dominates despite its global average being near zero. The primary role of this conversion, which reflects ageostrophic circulation, is to compensate for a large part of the mean diabatic heating. This is not obvious from Lorenz's formulation.

- Advection terms of the mean and eddy APE are obscured in the globally integrated framework. Nevertheless, it is shown here that advection of the mean APE is essential for providing APE into (and increasing baroclinicity within) the storm tracks, rather than APE being generated diabatically in situ by processes, such as SST heating.
- The mean APE advection is primarily from latitudes poleward of the storm tracks, which may have implications on the latitudinal extent of storm tracks. It was shown in Novak et al. (2015) that the equatorward part of the North Atlantic storm track is anchored near the latitude of the subtropical jet. This can be explained by the Hadley cell edge being anchored by a tropical energy balance (Mbengue and Schneider 2018). However, Novak et al. (2015) also find that the poleward edge of storm tracks is much more transient, which may be because the advection of cold temperatures determines the

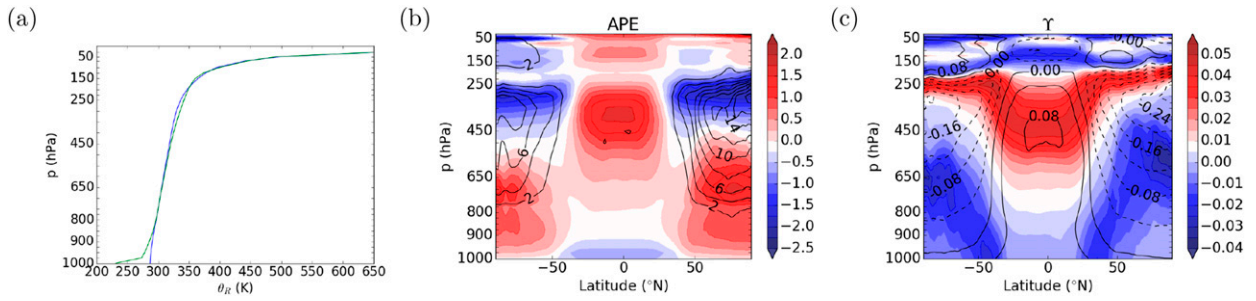


FIG. A1. Comparison of the quicksort [green line in (a) and black contours in (b) and (c)] to isobaric averaging [blue line in (a) and shading in (b) and (c) displayed as difference from when using the quicksort method] methods to define (a) the reference potential temperature profiles. The resultant effect on (b) the local APE ($10^5$ J m$^{-2}$) and (c) thermal efficiency. Data used are from 1 Jan 2000.

extent to which eddies can grow and propagate poleward.

- The analysis above revealed an interesting variability of APE density in the upper-level troposphere over Greenland. The variabilities of mean APE density and thermal efficiency exhibit an interhemispheric wave train that emanates from the ENSO region and propagates into the higher latitudes. The wave train in the Southern Hemisphere reaches the Ross Sea, and the variability may be even more prominent in the winter. With Greenland and Ross Sea being predicted to experience large changes in their land ice and sea ice coverage (Jacobs et al. 2002; Shepherd and Wingham 2007; Jacobs et al. 2011), it is possible that these regions of main supply of mean APE into storm tracks will play an important role in midlatitude dynamics in the future climate.

We are keen to emphasize that these are merely a few illustrations of the usefulness of the local APE density as an atmospheric diagnostic. For a thorough specific analysis of storm tracks, one may wish to optimize the choices of the reference state and separation methods into eddy and mean quantities. The choices made here are primarily to facilitate comparison with existing studies. The APE density framework can be further extended to a multicomponent fluid (Bannon 2005; Tailleux 2013b; Peng et al. 2015; Tailleux 2018). However, the addition of moisture would introduce the possibility of parcels possessing multiple reference states. This would affect the magnitude of APE and most likely increase it (Lorenz 1979; Pauluis and Held 2002; Bannon 2005). Peng et al. (2015) presented an application of a positive-definite definition of the moist local APE based on using the virtual temperature in an idealized atmosphere and showed the marked difference between using the classical exergy and their APE density. However, such considerations are beyond the scope of this paper, which demonstrates the usefulness of this local framework in analyzing large-scale dynamics and provides interesting directions for further focused research.

*Acknowledgments.* Lenka Novak is supported by the U.K. Natural Environment Research Council (Grant NE/M014932/1). We thank Prof. Tapio Schneider for a useful discussion on APE and Dr. Fred Kucharski for his helpful suggestions on clarifying the manuscript.

## APPENDIX A

### Two Methods for Constructing the Reference Potential Temperature

The first method uses parcel sorting. For each time the global potential temperature is divided into parcels. For example, the ERA-Interim dataset has a resolution of 512 longitude values, 256 latitude values, and 37 pressure levels, giving 4 849 664 parcels. These parcels were then sorted using the "quicksort" sorting algorithm for higher numerical efficiency. In this sorted order each parcel mass was then draped across Earth's surface yielding the height of each parcel. The result is $\theta_r$ as a function of the cumulative parcel mass (which can be readily converted to pressure). The $\theta_r$ profile for the required pressure levels of the dataset was then obtained using linear interpolation.

The second method is using the latitudinally weighted isobaric averaging as was used by Lorenz (1955b) and others. This method is faster, as discussed in the text.

The quicksort and isobaric averaging methods are compared here for 1 January 2000 in ERA-Interim. Their $\theta_r$ profiles and the zonally averaged APE and thermal efficiencies are shown in Fig. A1. In the zonal-mean plots, the quantities derived using the isobaric averaging are shown as anomalies from those derived using the quicksort method.

The $\theta_r$ two profiles are almost equivalent apart from the very low levels and near the tropopause. This makes a

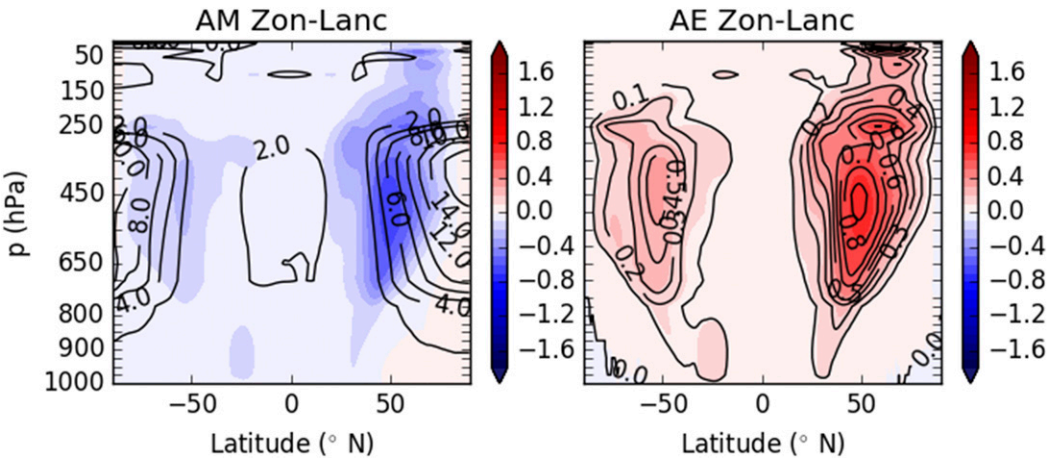


FIG. B1. Differences between the (left) mean and (right) eddy APE fields ($10^5$ J m$^{-2}$) of the zonal-mean-based and Lanczos-based frameworks (shading). The black contours show the zonal-mean-based APE components for reference.

small difference in the APE, with the quicksort yielding a lower APE in the tropics and low-level polar regions and higher APE in the upper-level polar regions. The quicksort method also produces a lower thermal efficiency near the tropopause and higher elsewhere.

One could argue the quicksort method is more accurate. However, given the data resolution, we are only interested in the larger-scale patterns in the energy and conversion terms. The smoother reference potential temperature profile is therefore still adequate, and it allows a more direct comparison with the existing literature. In addition, the quicksort method relies on all potential temperature values, including those in the highest levels, which are often not well constrained.

## APPENDIX B

### Eddy and Mean Local APE Using the Zonal-Mean- and Lanczos Filter–Based Frameworks

It is noted that the zonal-mean-based framework is qualitatively similar to the Lanczos-based framework, as shown in Fig. B1. As expected, a part of the midlatitude eddies (low-frequency and stationary eddies) is transferred from the eddy component to the mean component in the Lanczos-based framework. The mean APE mirrors closely the distribution of the total APE, so only the former is presented here.

## REFERENCES

Ahbe, E., and K. Caldeira, 2017: Spatial distribution of generation of Lorenz's available potential energy in a global climate model. *J. Climate*, **30**, 2089–2101, https://doi.org/10.1175/JCLI-D-15-0614.1.

Andrews, D. G., 1981: A note on potential energy density in a stratified compressible fluid. *J. Fluid Mech.*, **107**, 227–236, https://doi.org/10.1017/S0022112081001754.

Bannon, P. R., 2005: Eulerian available energetics in moist atmospheres. *J. Atmos. Sci.*, **62**, 4238–4252, https://doi.org/10.1175/JAS3516.1.

Blackburn, M., 1983: An energetic analysis of the general atmospheric circulation. Ph.D. thesis, University of Reading, 300 pp.

Codoban, S., and T. G. Shepherd, 2003: Energetics of a symmetric circulation including momentum constraints. *J. Atmos. Sci.*, **60**, 2019–2028, https://doi.org/10.1175/1520-0469(2003)060<2019:EOASCI>2.0.CO;2.

Duchon, C. E., 1979: Lanczos filtering in one and two dimensions. *J. Appl. Meteor.*, **18**, 1016–1022, https://doi.org/10.1175/1520-0450(1979)018<1016:LFIOAT>2.0.CO;2.

Dutton, J. A., 1973: The global thermodynamics of atmospheric motion. *Tellus*, **25**, 89–110, https://doi.org/10.3402/tellusa.v25i2.9647.

Eady, E. T., 1949: Long waves and cyclone waves. *Tellus*, **1**, 33–52, https://doi.org/10.3402/tellusa.v1i3.8507.

Emanuel, K. A., 1994: *Atmospheric Convection.* Oxford University Press, 580 pp.

Grotjahn, R., 1993: *Global Atmospheric Circulations: Observations and Theories.* Oxford University Press, 430 pp.

Hernadez-Deckers, D., and J. von Storch, 2010: Energetics responses to increases in greenhouse gas concentration. *J. Atmos. Sci.*, **23**, 3874–3887.

Holliday, D., and M. E. McIntyre, 1981: On potential energy density in an incompressible stratified fluid. *J. Fluid Mech.*, **107**, 221–225, https://doi.org/10.1017/S0022112081001742.

Hoskins, B. J., and P. J. Valdes, 1990: On the existence of storm-tracks. *J. Atmos. Sci.*, **47**, 1854–1864, https://doi.org/10.1175/1520-0469(1990)047<1854:OTEOST>2.0.CO;2.

——, I. N. James, and G. H. White, 1983: The shape, propagation and mean-flow interaction of large-scale weather systems. *J. Atmos. Sci.*, **40**, 1595–1612, https://doi.org/10.1175/1520-0469(1983)040<1595:TSPAMF>2.0.CO;2.

Hu, Q., Y. Tawaye, and S. Feng, 2004: Variations of the Northern Hemisphere atmospheric energetics: 1948–2000. *J. Climate*, **17**, 1975–1986, https://doi.org/10.1175/1520-0442(2004)017<1975:VOTNHA>2.0.CO;2.

Jacobs, S. S., C. F. Giulivi, and P. A. Mele, 2002: Freshening of the Ross Sea during the late 20th century. *Science*, **297**, 386–389, https://doi.org/10.1126/science.1069574.

——, A. Jenkins, C. F. Giulivi, and P. Dutrieux, 2011: Stronger ocean circulation and increased melting under Pine Island Glacier ice shelf. *Nat. Geosci.*, **4**, 519–523, https://doi.org/10.1038/ngeo1188.

James, I. N., 1994: *Introduction to Circulating Atmospheres.* Cambridge University Press, 230 pp.

Johnson, D. R., 1970: The available potential energy of storms. *J. Atmos. Sci.*, **27**, 727–741, https://doi.org/10.1175/1520-0469(1970)027<0727:TAPEOS>2.0.CO;2.

Kållberg, P., P. Berrisford, B. Hoskins, A. Simmmons, S. Uppala, S. Lamy-Thépaut, and R. Hine, 2005: ERA-40 Atlas. ERA-40 Project Rep. Series 19, ECMWF, 199 pp.

Karlsson, S., 1997: Energy, entropy, and exergy in the atmosphere. Ph.D. thesis, Chalmers University of Technology, 121 pp.

Kaspi, Y., and T. Schneider, 2013: The role of stationary eddies in shaping midlatitude storm tracks. *J. Atmos. Sci.*, **70**, 2596–2613, https://doi.org/10.1175/JAS-D-12-082.1.

Kucharski, F., 1997: On the concept of exergy and available potential energy. *Quart. J. Roy. Meteor. Soc.*, **123**, 2141–2156, https://doi.org/10.1002/qj.49712354317.

——, and A. J. Thorpe, 2000: Local energetics of an idealized baroclinic wave using extended exergy. *J. Atmos. Sci.*, **57**, 3272–3284, https://doi.org/10.1175/1520-0469(2000)057<3272:LEOAIB>2.0.CO;2.

Li, L., A. P. Ingersoll, X. Jiang, D. Feldman, and Y. L. Yung, 2007: Lorenz energy cycle of the global atmosphere based on reanalysis datasets. *Geophys. Res. Lett.*, **34**, L16813, https://doi.org/10.1029/2007GL029985.

Lorenz, E. N., 1955a: Generation of available potential energy and the intensity of the general circulation. University of California, Los Angeles, Dept. of Meteorology Tech. Rep. 1, 36 pp.

——, 1955b: Available potential energy and the maintenance of the general circulation. *Tellus*, **7**, 157–167, https://doi.org/10.3402/tellusa.v7i2.8796.

——, 1979: Numerical evaluation of moist available energy. *Tellus*, **31**, 230–235, https://doi.org/10.3402/tellusa.v31i3.10429.

Mbengue, C., and T. Schneider, 2017: Storm-track shifts under climate change: Toward a mechanistic understanding using baroclinic mean available potential energy. *J. Atmos. Sci.*, **74**, 93–110, https://doi.org/10.1175/JAS-D-15-0267.1.

——, and ——, 2018: Linking Hadley circulation and storm tracks in a conceptual model of the atmospheric energy balance. *J. Atmos. Sci.*, **75**, 841–856, https://doi.org/10.1175/JAS-D-17-0098.1.

Novak, L., M. H. P. Ambaum, and R. Tailleux, 2015: The lifecycle of the North Atlantic storm track. *J. Atmos. Sci.*, **72**, 821–833, https://doi.org/10.1175/JAS-D-14-0082.1.

O'Gorman, P. A., and T. Schneider, 2008: Energy of midlatitude transient eddies in idealized simulations of changed climates. *J. Climate*, **21**, 5797–5806, https://doi.org/10.1175/2008JCLI2099.1.

Oort, A. H., 1964: On estimates of the atmospheric energy cycle. *Mon. Wea. Rev.*, **92**, https://doi.org/10.1175/1520-0493(1964)092<0483:OEOTAE>2.3.CO;2.

Pauluis, O., and I. M. Held, 2002: Entropy budget of an atmosphere in radiative–convective equilibrium. Part II: Latent heat transport and moist processes. *J. Atmos. Sci.*, **59**, 140–149, https://doi.org/10.1175/1520-0469(2002)059<0140:EBOAAI>2.0.CO;2.

Pavan, V., N. Hall, P. Valdes, and M. Blackburn, 1999: The importance of moisture distribution for the growth and energetics of mid-latitude systems. *Ann. Geophys.*, **17**, 242–256, https://doi.org/10.1007/s00585-999-0242-y.

Pearce, R., 1978: On the concept of available potential energy. *Quart. J. Roy. Meteor. Soc.*, **104**, 737–755, https://doi.org/10.1002/qj.49710444115.

Pedlosky, J., 1992: *Geophysical Fluid Dynamics.* Springer, 230 pp.

Peng, J., L. Zhang, and Y. Zhang, 2015: On the local available energetics in a moist compressible atmosphere. *J. Atmos. Sci.*, **72**, 1521–1561, https://doi.org/10.1175/JAS-D-14-0181.1.

Saenz, J. A., R. Tailleux, E. D. Butler, G. O. Hughes, and K. I. Oliver, 2015: Estimating Lorenz's reference state in an ocean with a nonlinear equation of state for seawater. *J. Phys. Oceanogr.*, **45**, 1242–1257, https://doi.org/10.1175/JPO-D-14-0105.1.

Schneider, T., and C. C. Walker, 2008: Scaling laws and regime transitions of macroturbulence in dry atmospheres. *J. Atmos. Sci.*, **65**, 2153–2173, https://doi.org/10.1175/2007JAS2616.1.

Scotti, A., and B. White, 2014: Diagnosing mixing in stratified turbulent flows with a locally defined available potential energy. *J. Fluid Mech.*, **740**, 114–135, https://doi.org/10.1017/jfm.2013.643.

Shepherd, A., and D. Wingham, 2007: Recent sea-level contributions of the Antarctic and Greenland ice sheets. *Science*, **315**, 1529–1532, https://doi.org/10.1126/science.1136776.

Shepherd, T. G., 1993: A unified theory of available potential energy. *Atmos.–Ocean*, **31**, 1–26, https://doi.org/10.1080/07055900.1993.9649460.

Siegmund, P., 1994: The generation of available potential energy, according to Lorenz' exact and approximate equation. *Tellus*, **46A**, 566–582, https://doi.org/10.3402/tellusa.v46i5.15645.

Simmons, A. J., and B. J. Hoskins, 1978: The lifecycle of some baroclinic waves. *J. Atmos. Sci.*, **35**, 414–432, https://doi.org/10.1175/1520-0469(1978)035<0414:TLCOSN>2.0.CO;2.

Tailleux, R., 2013a: Available potential energy and exergy in stratified fluids. *Annu. Rev. Fluid Mech.*, **45**, 35–58, https://doi.org/10.1146/annurev-fluid-011212-140620.

——, 2013b: Available potential energy density for a multicomponent Boussinesq fluid with arbitrary nonlinear equation of state. *J. Fluid Mech.*, **735**, 499–518, https://doi.org/10.1017/jfm.2013.509.

——, 2018: Local available energetics of multicomponent compressible stratified fluids. *J. Fluid Mech.*, **842**, R1, https://doi.org/10.1017/jfm.2018.196.

Veiga, J. A. P., and T. Ambrizzi, 2013: A global and hemispherical analysis of the Lorenz energetics based on the representative concentration pathways used in CMIP5. *Adv. Meteor.*, **2013**, 485047, http://dx.doi.org/10.1155/2013/485047.

von Storch, J., C. Eden, I. Fast, H. Haak, D. Hernández-Deckers, E. Maier-Reimer, J. Marotzke, and D. Stammer, 2012: An estimate of the Lorenz energy cycle for the world ocean based on the STORM/NCEP simulation. *J. Phys. Oceanogr.*, **42**, 2185–2205, https://doi.org/10.1175/JPO-D-12-079.1.

Young, W. R., 2012: An exact thickness-weighted average formulation of the Boussinesq equations. *J. Phys. Oceanogr.*, **42**, 692–707, https://doi.org/10.1175/JPO-D-11-0102.1.

Zemskova, V., B. L. White, and A. Scotti, 2015: Available potential energy and the general circulation: Partitioning wind, buoyancy forcing, and diapycnal mixing. *J. Phys. Oceanogr.*, **45**, 1510–1531, https://doi.org/10.1175/JPO-D-14-0043.1.